

Electrochemistry and structure of $\text{Li}_{2-x}\text{Cr}_y\text{Mn}_{2-y}\text{O}_4$ phases

I.J. Davidson ^{a,*}, R.S. McMillan ^a, H. Slegre ^a, B. Luan ^a, I. Kargina ^a, J.J. Murray ^a,
I.P. Swainson ^b

^a Institute for Chemical Process and Environmental Technology, National Research Council Canada, Montreal Road, Ottawa, Ontario, Canada K1A 0R6

^b Steacie Institute for Molecular Sciences, National Research Council Canada, Montreal Road, Ottawa, Ontario, Canada K1A 0R6

Abstract

The synthesis of phases in the solid state solution series $\text{Li}_2\text{Cr}_y\text{Mn}_{2-y}\text{O}_4$ where $0 < y < 2$ and their use as cathodes in lithium ion cells was reported previously [I.J. Davidson, R.S. McMillan, J.J. Murray, *J. Power Sources*, 54 (1995) 205–208]. This paper reports the results of electrochemical evaluations with metallic lithium anodes and on Rietveld refinements of X-ray and neutron powder diffraction data for these phases. Although these materials are prepared at moderately high temperatures, the refinements show that they have a structure similar to the monoclinic layered form of LiMnO_2 prepared by soft chemistry at low temperatures by Armstrong and Bruce [A.R. Armstrong, P.G. Bruce, *Nature*, 381 (1996) 499–500] and by Delmas and Capitaine [C. Delmas, F. Capitaine, *Extended Abstracts of the Eighth International Meeting on Lithium Batteries* (1996) 470–471]. The degree of monoclinic distortion in the initial materials has an effect on the structural changes that occur on charging. The phases with a small monoclinic distortion change to an undistorted hexagonal structure on their first charge while those with a large monoclinic distortion change to a spinel-like structure on cycling. Crown Copyright © 1999 Published by Elsevier Science S.A. All rights reserved.

Keywords: $\text{Li}_2\text{Cr}_y\text{Mn}_{2-y}\text{O}_4$; Electrochemistry; Structure

1. Introduction

A high level of global effort has been applied to the search for positive electrode materials for lithium ion batteries that combine high operating voltage with high capacity and rate. Electrochemical assessment of cathodes based on phases of the solid state solution, $\text{Li}_2\text{Cr}_y\text{Mn}_{2-y}\text{O}_4$, demonstrates reversible capacities which although large are much less than the theoretical maximum. Structural studies on a broad range of compositions of $\text{Li}_2\text{Cr}_y\text{Mn}_{2-y}\text{O}_4$ both as prepared and after electrochemical cycling have identified the structural transitions which occur in these materials and provided a better understanding of their electrochemical behavior. As reported previously single-phase materials can be obtained for compositions from $\text{Li}_2\text{Cr}_{0.1}\text{Mn}_{1.9}\text{O}_4$ to $\text{Li}_2\text{Cr}_{1.9}\text{Mn}_{0.1}\text{O}_4$. Crystallographic structures refined by Rietveld profile analysis of the X-ray diffraction patterns confirm that the structure of compositions with a static Jahn–Teller distortion belong to the space group $C2/m$ as was pointed out by Dahn et al. [1]. The effect of dilution of the Jahn–Teller ion, Mn^{3+} , by Cr^{3+} substitution causes a regular decrease in the degree

of monoclinic distortion with increasing Cr^{3+} composition. Phases in the series $\text{Li}_2\text{Cr}_y\text{Mn}_{2-y}\text{O}_4$ in which $y \geq 1.4$ containing 30 mol%, or less, manganese also have a layered structure but the symmetry is increased to hexagonal by the absence of a cooperative Jahn–Teller distortion.

Fabrication of lithium ion batteries with positive electrodes based on $\text{Li}_2\text{Cr}_y\text{Mn}_{2-y}\text{O}_4$ was demonstrated in an earlier publication [2]. The availability of more oxidatively stable electrolytes has permitted the study of cathodes based on these materials to higher voltages than previously reported. The $\text{Li}_2\text{Cr}_y\text{Mn}_{2-y}\text{O}_4$ cathodes were assessed in cells with metallic lithium anodes to clarify their electrochemistry.

2. Experimental

$\text{Li}_2\text{Cr}_y\text{Mn}_{2-y}\text{O}_4$ phases were prepared from stoichiometric mixtures of either: (a) Li_2CO_3 (Aldrich 99.997), Cr_2O_3 (Fisher Certified Reagent), and MnO_2 (Fisher Certified Reagent), or (b) $\text{LiOH} \cdot \text{H}_2\text{O}$ (Aldrich 99.9%), Mn_2O_3 (Aldrich 99.9%) and Cr_2O_3 (Aldrich 99.9%). The intimately ground powders were loaded into alumina crucibles and then heat treated in tube furnaces under a flow of argon gas. They were first calcined for 3 h at 650°C for

* Corresponding author

mixtures containing Li_2CO_3 or at 450°C for those with $\text{LiOH} \cdot \text{H}_2\text{O}$ and then fired at 1000°C for a further 24 h. Often more than one firing at 1000°C was required to obtain a single-phase product. The samples were reground between firings.

A Scintag XDS 2000 with a theta–theta geometry and a copper X-ray tube was used to obtain the X-ray data. The diffractometer has a pyrolytic graphite monochromator in front of the detector. The samples were mounted on a zero background sample holder made from an oriented silicon wafer. In some cases, X-ray powder diffraction patterns were obtained on cathodes extracted from previously cycled coin cells. The coin cells were opened on a small lathe to prevent shorting. The air sensitive samples were removed from the cells in a helium filled dry box and heat sealed in a polyethylene bag for the diffraction studies. Lattice parameters were calculated from the measured peak positions with the program TREOR [3]. Relative intensities of peaks were obtained by profile fitting to a Pearson VII curve shape.

More detailed structures were obtained by Rietveld profile analysis of some of the X-ray powder diffraction patterns. The computer program RIETAN (Izumi) [4] was used for the structure refinements. The program GSAS [5] was used to refine structural parameters from neutron powder diffraction data. The neutron diffraction experiments were conducted on the C2 neutron powder diffractometer at the Chalk River Laboratories NRU reactor. The instrument consists of an 800-wire detector spanning 80° in 2θ . Measurements were made up to 117° in 2θ by merging a low-angle and a high-angle measurement.

The electrochemical cycling was done in 2325 coin cells with an internal spring and spacer to maintain an adequate pressure on the electrode stack. The cathodes were punched from a cast made on aluminum foil by a doctor blade technique using a slurry in *n*-methyl pyrrolidone which contained active material, Super S carbon black, and PVDF binder in a weight ratio of 85:10:5. The cathodes have a diameter of 1.27 cm and thickness ranging from 0.08 to 0.20 mm. The anodes were lithium foil (Foote Mineral) disks of 1.65 cm diameter and 0.05 cm thickness. Two sheets of Celgard 3501 microporous polypropylene formed the separator. A 1 M LiPF_6 solution in 1:1 ratio of

ethylene carbonate/dimethyl carbonate from Mitsubishi Chemical was used as the electrolyte. The cell were assembled and crimped in a helium filled glove box. The assembled cell were cycled galvanostatically at 3.6 mA/g between voltage limits of 4.5 and 2.5 V on custom built cell cyclers.

3. Results and discussion

3.1. Structural details

The crystallographic structures of single-phase compositions of $\text{Li}_2\text{Cr}_y\text{Mn}_{2-y}\text{O}_4$ were investigated by powder X-ray diffraction. Some of the diffraction patterns were used for Rietveld structure refinements. A change of symmetry occurs from hexagonal to monoclinic occurs between the compositions $\text{Li}_2\text{Cr}_{1.4}\text{Mn}_{0.6}\text{O}_4$ and $\text{Li}_2\text{Cr}_{1.3}\text{Mn}_{0.7}\text{O}_4$. The extinctions and relative intensities of X-ray powder patterns are consistent with the hexagonal phases having a 3R-type structure like LiCrO_2 and the monoclinic phases having a layered LiMnO_2 type structure.

The hexagonal and monoclinic unit cells differ mainly in the relative positioning of the layers perpendicular to the *c*-axis. The layered form of LiMnO_2 prepared by low-temperature ion exchange of NaMnO_2 is monoclinic rather than hexagonal because of a cooperative Jahn–Teller distortion caused by the Mn^{3+} ion. Within the compositions of $\text{Li}_2\text{Cr}_y\text{Mn}_{2-y}\text{O}_4$ with monoclinic structures, the dilution of the effect of the Jahn–Teller ion, Mn^{3+} , by Cr^{3+} substitution causes a regular decrease in the degree of monoclinic distortion with increasing Cr^{3+} composition. Table 1 lists the crystallographic lattice parameters for the range of compositions studied.

Neutron powder diffraction is a useful complement to X-ray powder diffraction in studying cathode materials. In that while lithium atoms are weak scatterers of X-rays, they have a large and negative scattering length for neutrons. The neutron scattering lengths of the first row transition metal atoms vary widely. Consequently, neutron powder diffraction is very useful for determining the relative cation occupancies and ordering in quaternary metal

Table 1
Crystallographic dimensions of $\text{Li}_2\text{Cr}_y\text{Mn}_{2-y}\text{O}_4$ for $0.1 \leq y \leq 1.9$

Composition	<i>a</i> (Å)	<i>b</i> (Å)	<i>c</i> (Å)	β (degrees)	Space group	Volume (Å ³)
$\text{Li}_2\text{Cr}_{0.1}\text{Mn}_{1.9}\text{O}_4$	5.4370 (9)	2.8106 (3)	5.390 (1)	115.94 (1)	<i>C2/m</i>	74.07
$\text{Li}_2\text{Cr}_{0.25}\text{Mn}_{1.75}\text{O}_4$	5.390 (1)	2.8209 (4)	5.368 (2)	115.31 (2)	<i>C2/m</i>	73.72
$\text{Li}_2\text{Cr}_{0.5}\text{Mn}_{1.5}\text{O}_4$	5.353 (3)	2.8300 (9)	5.328 (4)	114.61 (4)	<i>C2/m</i>	73.39
$\text{Li}_2\text{CrMnO}_4$	5.197 (1)	2.8616 (5)	5.213 (2)	112.17 (2)	<i>C2/m</i>	71.79
$\text{Li}_2\text{Cr}_{1.25}\text{Mn}_{0.75}\text{O}_4$	5.1420 (9)	2.8744 (3)	5.1777 (9)	111.27 (1)	<i>C2/m</i>	71.31
$\text{Li}_2\text{Cr}_{1.5}\text{Mn}_{0.5}\text{O}_4$	2.909 (2)		14.442 (5)		<i>R-3m</i>	70.56
$\text{Li}_2\text{Cr}_{1.75}\text{Mn}_{0.25}\text{O}_4$	2.9042 (9)		14.432 (4)		<i>R-3m</i>	70.28
$\text{Li}_2\text{Cr}_{1.8}\text{Mn}_{0.2}\text{O}_4$	2.902 (1)		14.428 (4)		<i>R-3m</i>	70.15
$\text{Li}_2\text{Cr}_{1.9}\text{Mn}_{0.1}\text{O}_4$	2.899 (1)		14.431 (5)		<i>R-3m</i>	70.02

Table 2
Summary of Rietveld refinement of neutron powder diffraction data for two samples of $\text{Li}_2\text{Cr}_{0.1}\text{Mn}_{1.9}\text{O}_4$

Sample a—from Li_2CO_3 , Cr_2O_3 and MnO_2				
Lattice parameters				
<i>a</i>	<i>b</i>	<i>c</i>	β	
5.428(2)	2.8115(8)	5.388(2)	115.834(3)	
Atomic parameters				
Atom	<i>x</i>	<i>y</i>	<i>z</i>	%
Li	0	1/2	1/2	1
Mn	0	0	0	0.94(1)
Cr	0	0	0	0.06(1)
O	0.2699(5)	0	0.7705(4)	1
<i>R</i> -factors				
<i>wRp</i> = 0.0381		<i>Rp</i> = 0.0255		
Sample b — $\text{LiOH} \cdot \text{H}_2\text{O}$, Cr_2O_3 and Mn_2O_3				
Lattice parameters				
<i>a</i>	<i>b</i>	<i>c</i>	β	
5.4321(2)	2.8093(1)	5.3826(2)	115.927(1)	
Atomic parameters				
Atom	<i>x</i>	<i>y</i>	<i>z</i>	%
Li	0	1/2	1/2	1
Mn	0	0	0	0.97(1)
Cr	0	0	0	0.03(1)
O	0.2715(3)	0	0.7705(3)	1
<i>R</i> -factors				
<i>wRp</i> = 0.0517		<i>Rp</i> = 0.0360		

oxides. In addition, refinement of anisotropic thermal parameters from neutron powder diffraction data can be used to study lithium ion mobility. Neutron diffraction studies were conducted on two samples of $\text{Li}_2\text{Cr}_{0.1}\text{Mn}_{1.9}\text{O}_4$: one

prepared from Li_2CO_3 , Cr_2O_3 and MnO_2 and the other from $\text{LiOH} \cdot \text{H}_2\text{O}$, Cr_2O_3 and Mn_2O_3 . A Rietveld refinement of the diffraction patterns indicated that the samples differed slightly in the lengths of their *a*-axis but were otherwise very similar. The absence of additional reflections confirmed that both samples exhibit a high degree of purity. The results of the structure refinements are summarized in Table 2. The model used to refine both samples was one in which the Li was fully ordered on the position (0,1/2,1/2), and the O was free to move in (*x*,0,*z*). Mn–Cr exchange was left as a free, parameter, with the only constraint that the site must be fully occupied by either Mn or Cr. Refinements were also tried in which the fraction of Cr was constrained to be 5% on (0,0,0), and this made little effect on the refined values. The most interesting observation from the refinements is the high degree of anisotropy in the thermal parameters of the lithium atoms. $\text{Li}_2\text{Cr}_{0.1}\text{Mn}_{1.9}\text{O}_4$ has a layered structure in which it might be expected that the lithium atoms have freedom of motion in two-dimensions. However, the thermal parameters, shown in Fig. 1, clearly indicate that the lithium ion mobility is largely restricted to the direction of the *a*-axis. The small difference in the length of the *a*-axis between the samples also suggests that it is very sensitive to small variations in composition.

3.2. Electrochemical characterization

Fig. 2 is a plot of charge and discharge curves for the first three cycles of coin cells with $\text{Li}_2\text{Cr}_y\text{Mn}_{2-y}\text{O}_4$ cathodes and metallic lithium anodes. Lithium anodes simplify

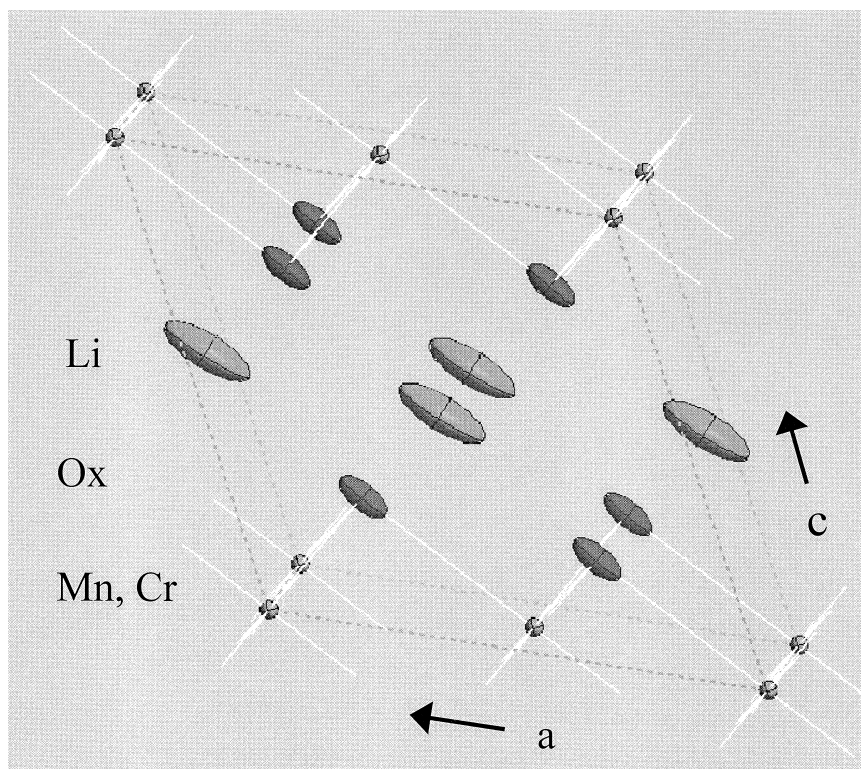


Fig. 1. Anisotropic thermal parameters for $\text{Li}_2\text{Cr}_{0.1}\text{Mn}_{1.9}\text{O}_4$ as refined from neutron powder diffraction data.

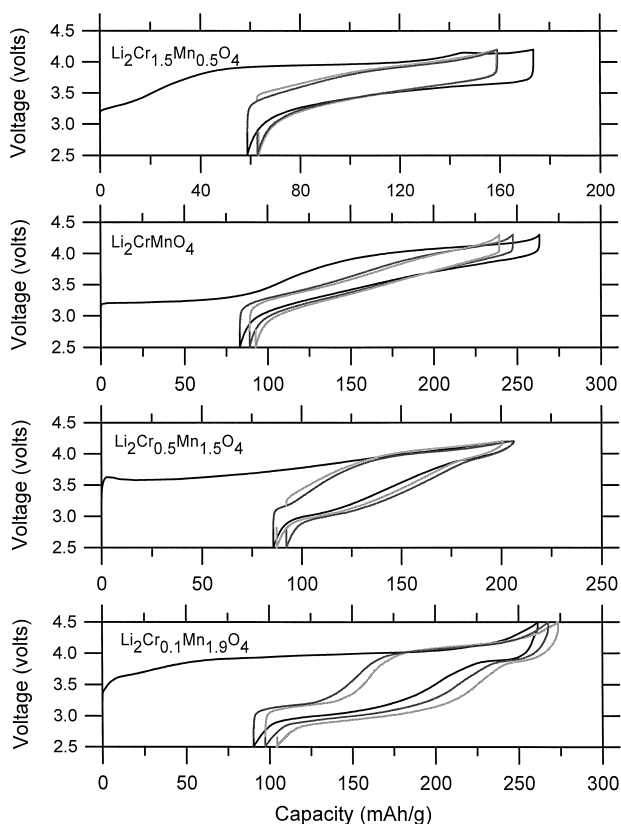


Fig. 2. Charge and discharge curves for the first three cycles of $\text{Li}_2\text{Cr}_y\text{Mn}_{2-y}\text{O}_4$ cathodes cycled at 3.6 mA/g between 2.5 V and 4.2 V for $y = 1.5$ and 0.5, 4.3 V for $y = 1.0$, and 4.5 V for $y = 0.1$.

the interpretation of the potential versus capacity curves because the potential of the anode remains constant. Consequently, the observed changes in the potential reflect changes in lithium ion activity in the cathode as a function of its lithium composition. The four compositions shown represent the range electrochemical behavior observed in $\text{Li}_2\text{Cr}_y\text{Mn}_{2-y}\text{O}_4$ cathodes. All compositions show a capacity loss between the first charge and the first discharge. The first cycle coulombic inefficiency must be due to limitations in the cathodes, as the reversibility of the lithium electrode is not limiting.

The shape of the first charge curves for the compositions with $y \leq 0.5$ are different from that of subsequent cycles. This indicates that a phase transition is occurring on the first charge. Subsequent cycles show a step in the voltage curve similar to that observed for spinel-related $\lambda\text{-Li}_2\text{Mn}_2\text{O}_4$. The severity of the step is dependent on the Mn/Cr ratio and increases with increasing manganese content. The voltage versus capacity plots for cells containing $\text{Li}_2\text{Cr}_{0.5}\text{Mn}_{1.5}\text{O}_4$ and $\text{Li}_2\text{Cr}_{0.1}\text{Mn}_{1.9}\text{O}_4$ cathodes represent the two extremes of behavior. The severity of the voltage step scales with degree of Jahn–Teller distortion in the initial material. Ex-situ X-ray diffraction studies of cycled cathodes confirm that a structure change has occurred. Fig. 3 is the X-ray diffraction pattern of a $\text{Li}_{2-x}\text{Cr}_{0.2}\text{Mn}_{1.8}\text{O}_4$ cathode after it was charged to 4.4 V. Three of the peaks, near 45, 65 and 78 degrees, possibly contain overlapping contributions from the aluminum foil backing. The pattern can be indexed to a cubic

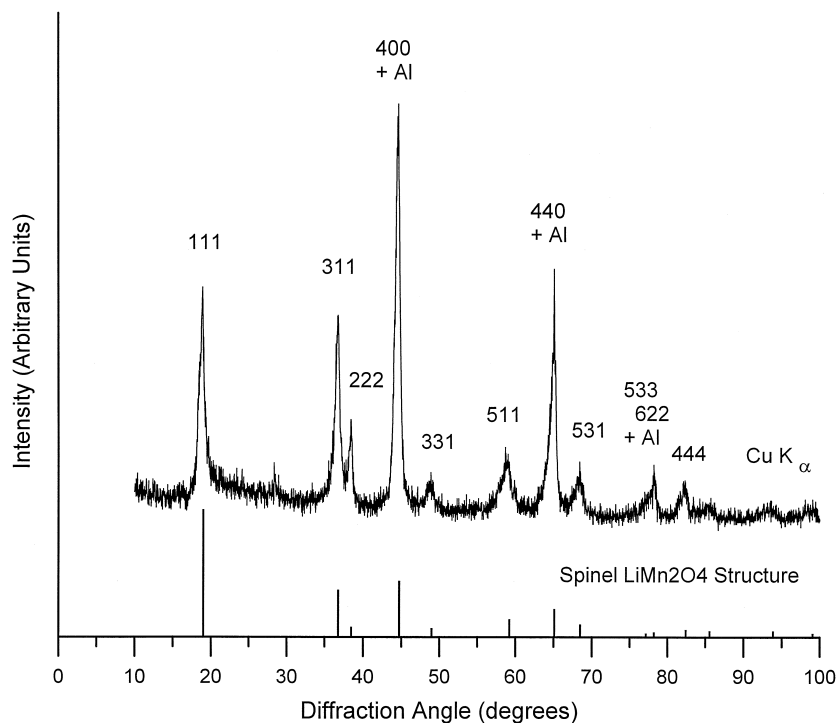


Fig. 3. X-ray powder diffraction pattern of a $\text{Li}_{2-x}\text{Cr}_{0.2}\text{Mn}_{1.8}\text{O}_4$ cathode after charging to 4.4 V and model calculation based on LiMn_2O_4 structure and a lattice parameter of 8.1 Å.

unit cell of lattice dimension 8.1 Å. The bar diagram below represents the calculated positions and intensities of a model based on the spinel LiMn_2O_4 structure with the observed unit cell dimensions.

Charging cathodes based on $\text{Li}_2\text{Cr}_y\text{Mn}_{2-y}\text{O}_4$ phases decreases the concentration of the Jahn–Teller ion, Mn^{3+} , by oxidizing it to Mn^{4+} . This causes a collapse of the cooperative Jahn–Teller distortion as evidenced by the site symmetry of the transition metal cations changing from D_{4h} to O_h and the crystallographic symmetry changing from monoclinic to hexagonal. Fig. 4 shows the X-ray diffraction patterns of $\text{Li}_2\text{CrMnO}_4$ cathodes after charging to particular capacities. The patterns also have contributions from the polyethylene film that was used to protect them from reaction with air during the diffraction measurement. These peaks are marked with asterisks and the one near 36° in 2θ overlaps with a diffraction peak of the cathode. Before electrochemically cycling $\text{Li}_2\text{CrMnO}_4$, it has a monoclinic structure. After charging a $\text{Li}_2\text{CrMnO}_4$ cathode to a capacity of 100 mA h/g, the diffraction pattern corresponds to a hexagonal LiCrO_2 -type structure. On further charging to 230 mA h/g, or 4.3 V versus lithium metal, the hexagonal structure is maintained. The X-ray diffraction pattern of a $\text{Li}_2\text{CrMnO}_4$ cathode that was charged to only 25 mA h/g exhibits a coexistence of the initial monoclinic phase and a partially charged hexagonal phase. This capacity corresponds to a point part way through the initial flat plateau in the voltage curve. A flat plateau in a capacity versus voltage curve is characteristic of a two-phase region. The initial charging of a $\text{Li}_2\text{CrMnO}_4$ cathode proceeds via a first order phase transition which is

not very reversible and results in a coulombic inefficiency on the first cycle. The inflection in the voltage curve occurs near 75 mA h/g. This capacity corresponds to oxidation of about 26% of the transition metal cations from +3 to +4 oxidation states. The inflection in the voltage curve indicates the capacity at which concentration of the Jahn–Teller ion, Mn^{3+} , decreases to less than that required to support a static Jahn–Teller distortion. A static Jahn–Teller distortion is observed in $\text{Li}_2\text{Cr}_y\text{Mn}_{2-y}\text{O}_4$ compositions with $y < 1.4$. The occurrence of the structural transition after only 26% of the metal cations have been oxidized suggests that Mn^{3+} is oxidized preferentially before Cr^{3+} . Subsequently, the reaction proceeds by a second order phase transformation and the structure remains hexagonal as a compositional changes occur with the continuous lithium deintercalation. The capacity region over which a hexagonal structure is maintained is highly reversible. A second set of similar experiments with cathodes of composition $\text{Li}_2\text{Cr}_{0.75}\text{Mn}_{1.25}\text{O}_4$ showed very similar behavior. On charging, hexagonal structures were observed over the voltage range from 3.5 to 4.5 V. A hexagonal structure was also observed after charging a cell to 4.5 V and then discharging it to 2.5 V.

Compositions of $\text{Li}_2\text{Cr}_y\text{Mn}_{2-y}\text{O}_4$ with $y > 1.4$ are hexagonal and might therefore be expected to cycle well in a lithium battery. However, cells containing cathodes based on $\text{Li}_2\text{Cr}_y\text{Mn}_{2-y}\text{O}_4$ compositions with $y > 1.5$ show large impedance and poor capacity. The composition $\text{Li}_2\text{Cr}_{1.5}\text{Mn}_{0.5}\text{O}_4$ does cycle reasonably well as shown in Fig. 2, but it also has a large loss of capacity between the first charge and the first discharge. The cause of this

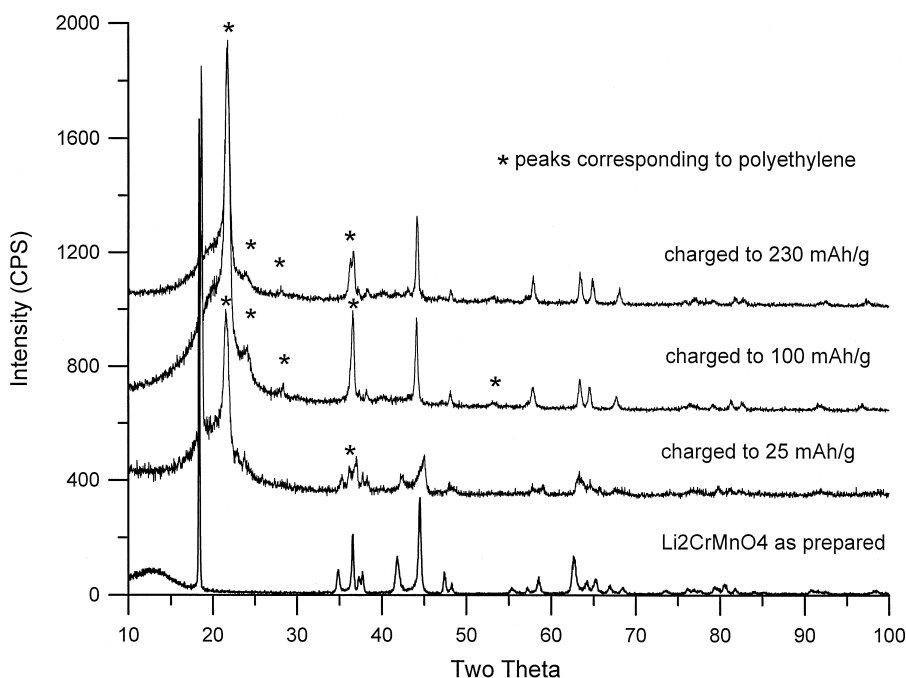


Fig. 4. X-ray powder diffraction patterns of $\text{Li}_2\text{CrMnO}_4$ cathodes before charging and after charging to 25, 100 and 230 mA h/g.

coulombic inefficiency is not obvious and requires further investigation.

4. Conclusions

X-ray diffraction studies on charged and discharge $\text{Li}_2\text{Cr}_y\text{Mn}_{2-y}\text{O}_4$ cathodes over a range of compositions were conducted to understand the structural changes that occur on cycling. These studies revealed that for compositions in which $y = 0.75, 1.0$ and 1.25 the first part of the charging process involves a first order phase transition between the monoclinic and hexagonal structures which is irreversible. Electrochemical evaluations of compositions in which $y \leq 0.5$ indicate a more dramatic in-situ structural change during the initial charge. X-ray diffraction examinations of cathodes based on compositions in which $y \leq 0.5$ suggest that these phases change to a spinel-related channel structure on the first charge. This transformation is similar to that observed for the layered and orthorhombic forms of LiMnO_2 .

Detailed studies on the electrochemistry and structural changes of cathodes containing $\text{Li}_2\text{CrMnO}_4$ during the first cycle were conducted. It was determined that the irreversible part of the first charge corresponds to a first order phase transition between the initial composition with a monoclinic structure and a partially charged composition with a hexagonal structure. All further cycling is associated with a highly reversible, second order phase transition in which hexagonal symmetry is maintained.

References

- [1] J.R. Dahn, T. Zheng, C.L. Thomas, *J. Electrochem. Soc.* 145 (1998) 851–859.
- [2] I.J. Davidson, R.S. McMillan, J.J. Murray, *J. Power Sources* 54 (1995) 205–208.
- [3] P.E. Werner, L. Eriksson, M. Westdahl, *J. Appl. Cryst.* 18 (1985) 367–370.
- [4] F. Izumi, *Rigaku J.* 6 (1) (1989) 10.
- [5] A.C. Larson, R.B. Von Dreele, GSAS-General Structure Analysis System, Copyright 1985–1994, Los Alamos National Laboratory.